# Partial valence-band spectra of Fe in $Cd_{1-x}Fe_xSe$

Reinhard Denecke and Lothar Ley
*Universität Erlangen-Nürnberg, Institut für Technische Physik II, D-8520 Erlangen, Federal Republic of Germany*

Jordi Fraxedas
*European Synchrotron Radiation Facility, F-38043 Grenoble, France*
(Received 8 September 1992)

We have studied the partial valence-band spectrum of Fe in $Cd_{1-x}Fe_xSe$ by exploiting the resonant enhancement of the Fe $3d$-derived features at the $3p$-$3d$ excitation threshold. Two resonance energies of 53.6 and 55.5 eV were detected by performing constant-initial-state measurements. The resonances correspond to transitions from the $3p^63d^6\,{}^5D$ ground state of the $Fe^{2+}$ ion to $3p^53d^7$ final states with $({}^5P,{}^5F)$ and ${}^5D$ symmetry, respectively. By taking difference spectra between energy-distribution curves measured on and off resonance, we obtained partial Fe $3d$-derived valence-band spectra that turned out to be quite different for the two resonance energies. In order to understand this difference and to derive ground-state properties from the valence-band spectra of the highly correlated Fe $3d$ system, a full-fledged configuration-interaction calculation for a $[FeSe_4]^{6-}$ cluster was performed. Taking the differences in coupling strength of the direct photoemission channels and the two core-excitation resonances into account, these model calculations reproduce the salient features of the partial valence-band spectra quite well. From this model calculation we obtain, among other things, a value for the Fe $3d$ correlation energy of about 7 eV. The ground state of Fe in $Cd_{1-x}Fe_xSe$ turns out to be describable in terms of 83% of the $|d^6\rangle$ configuration and 17% of the $|d^7\underline{L}\rangle$ configuration where an electron has been transferred from the ligand ($\underline{L}$) to the $3d$ shell. The effective number of electrons on the Fe atoms is thus calculated to be 6.16. To obtain an independent estimate of the correlation energy we also measured the Fe $2p$ core lines and modeled the spectrum with a calculation using again the configuration-interaction scheme in the cluster approximation. The best agreement between model and spectrum holds for a correlation energy of 5.5 eV, which is significantly smaller than the value derived from the valence-band spectra.

## I. INTRODUCTION

$Cd_{1-x}Fe_xSe$ is a member of the class of semiconductors called semimagnetic semiconductors. These are alloys of the II-VI family of semiconductors, in which a fraction of the group-II cations is replaced by transition-metal ions such as $Mn^{2+}$, $Fe^{2+}$, $Co^{2+}$, and others, while the zinc-blende or wurtzite structure of the parent crystal is maintained. The introduction of ions with large magnetic moments into the II-VI semiconductors leads to a number of magnetic phases which have been the focus of several studies.[1] It further induces a variety of magnetic phenomena such as a magnetic tunability of the band gap and a giant Faraday rotation,[2] which are not normally found in II-VI semiconductors. These effects rely, of course, on the hybridization of the moment carrying $d$ electrons on the transition metal with the $s$-$p$ electrons of the host lattice which make up the states at the band edges. For this reason, we are interested here in the degree of hybridization between the Fe $3d$ electrons and the Cd and Se-derived band states. To this end, we have determined the partial Fe $3d$-derived valence-band spectra by utilizing the selective resonance enhancement of these states via autoionization of the $3p^63d^6 \rightarrow 3p^53d^7$ Fe core excitation, a process normally referred to as resonant photoemission.

The electron-electron correlation within the Fe $3d$ shell which is responsible for the transfer of oscillator strength from the $3p \rightarrow 3d$ core excitation to the Fe $3d$ photoemission process prevents us, however, from a direct interpretation of the partial valence-band spectrum in terms of a ground-state density of states. Instead, we not only have to consider the different final-state multiplets which can be reached from the $d^6({}^5P)$ ground state of the $Fe^{2+}$ ion but also the covalency of the Fe-Se bonds which results in a noninteger average occupation of the Fe $3d$ shell. Both effects are modeled in a so-called configuration-interaction (CI) calculation of the $3d$ photoemission process.[3] We have applied this scheme to a $[FeSe_4]^{6-}$ cluster in which the $Fe^{2+}$ ion is tetrahedrally surrounded by four $Se^{2-}$ ions to mimic the nearest-neighbor environment of isolated $Fe^{2+}$ ions in $Cd_{1-x}Fe_xSe$.

The procedure is analogous to similar calculations performed earlier for the interpretation of the resonant photoemission spectra in $Cd_{1-x}Mn_xTe$.[4] The situation at hand differs, however, in one important aspect from that of $Cd_{1-x}Mn_xTe$. The $Mn^{2+}$ ion has no orbital angular momentum whereas the $Fe^{2+}$ ion possesses spin and orbital angular momenta of $S=2$ and $L=2$, respectively. This means that more than one multiplet state can be reached in the Fe $3p \rightarrow 3d$ core excitation. The different coupling strengths of the valence emission final states to

 

the core resonances are a major complication for the interpretation in the presented case.

The paper is organized as follows. Section II describes the experimental results, and the main aspects of the CI calculations are outlined in Sec. III. In Sec. IV, the partial valence-band spectrum is compared with the CI calculation and conclusions concerning the Fe $3d$ ground-state properties in $Cd_{1-x}Fe_xSe$ are drawn from this comparison and from the core-level spectra.

## II. EXPERIMENTAL RESULTS

The UV photoemission measurements were performed using synchrotron radiation from the storage ring BESSY (Berlin, Germany). Photon energies in the range from 10 to 130 eV were selected with a toroidal grating monochromator. The spectra were recorded with a toroidal energy analyzer (TEA) (Ref. 5) in the angle-integrating mode, with a resolution of about 0.2 eV.

The samples used were $Cd_{1-x}Fe_xSe$ crystals with Fe contents of 0%, 5%, and 10%. They had been grown by a modified Bridgman method at the Academy of Sciences in Warsaw.[6] To obtain clean surfaces, the samples were cleaved *in situ* in a vacuum of $2\times10^{-10}$ Torr.

Figure 1 shows a series of energy-distribution curves (EDC's) of $Cd_{0.95}Fe_{0.05}Se$ and $Cd_{0.9}Fe_{0.1}Se$ in the valence-band region for photon energies between 50 and 60 eV. The spectra have been corrected for higher-order emission from core levels, and they cover the top 7 eV of the valence bands. Deeper-lying states are obscured by emission from the Cd $4d$ core states at a binding energy of about 11 eV. At first glance, the spectra look essentially like the valence-band spectra of the CdSe host, as shown in the top panel of Fig. 1(b). But there are two new features: a small shoulder appears at the top of the valence bands in $Cd_{1-x}Fe_xSe$. Thus the width of the $Cd_{1-x}Fe_xSe$ valence bands is increased by about 1 eV. Since the other CdSe-derived features are not significantly changed in binding energy with respect to the vacuum level, the appearance of the shoulder leads to a shift of the valence-band maximum (VBM) (defined by extrapolating the leading edge of the first shoulder to the zero of intensity) by about 1 eV toward lower binding energy. Second, there appears a peak at a binding energy of about 3.9 eV, which is resonantly enhanced with a maximum near 55.4-eV photon energy.

In the following, we will concentrate on the samples where $x=0.1$. The energies of spectral features do not depend on the composition, but the intensities of the Fe-derived structures are of course very small for $x=0.05$.

In order to obtain more detailed information about the resonance energy, we measured constant-initial-state (CIS) spectra for initial states with various binding energies in the valence-band region, as is shown in Fig. 2. The features of interest are the two resonances which occur independently of the initial-state energy at fixed photon energies of 53.6 and 55.5 eV, respectively. A second-order Se $3d$ core emission which is of no concern here moves through the spectra on the left-hand side of Fig. 2. Due to the interference of the second-order core-level emission with the CIS spectra, the spectrum for $E_b=0.5$ eV had to be extracted from individual EDC's taken with closely spaced photon energies, after they had been corrected for the core line emission.

The two resonances are the sought after autoionization resonances, which couple to the Fe $3p\rightarrow3d$ core excitations and enhance the Fe $3d$ photoemission cross section at the resonance frequency. The resonances exhibit the typical Fano-profile, which stems from the interference of the discrete autoionization channel with the continuously varying cross section of the valence-band photoemission process.[7]

The fact that, in contrast to the Mn case, two reso-

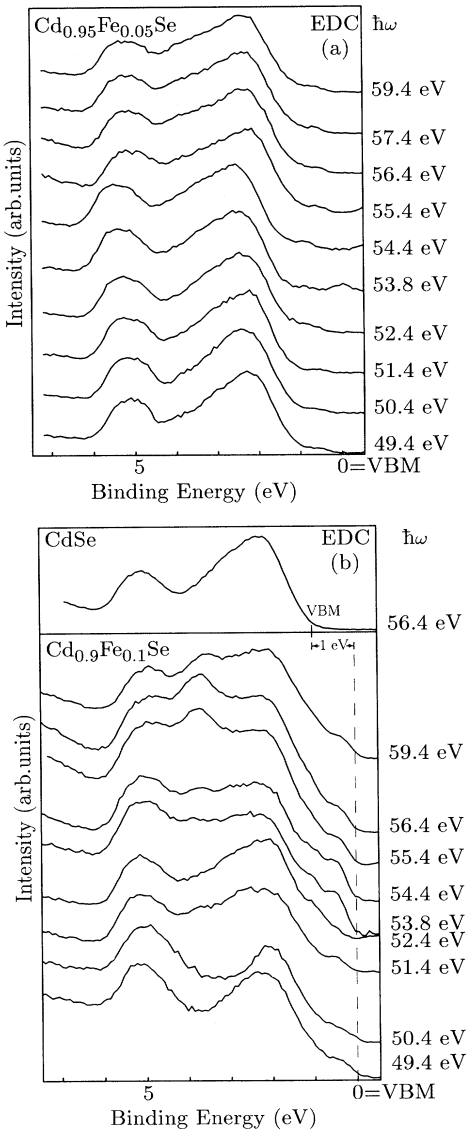


FIG. 1. Energy-distribution curves (EDC's) of (a) $Cd_{0.95}Fe_{0.05}Se$ and (b) $Cd_{0.9}Fe_{0.1}Se$. The binding energy zero is the valence-band maximum (VBM). The EDC's are shown for photon energies between 50 and 60 eV covering the Fe $3p$-$3d$ resonance energy at about 55.4 eV. The top panel in Fig. 1(b) shows a spectrum of CdSe for comparison; the two sets of spectra are aligned with respect to the vacuum level.

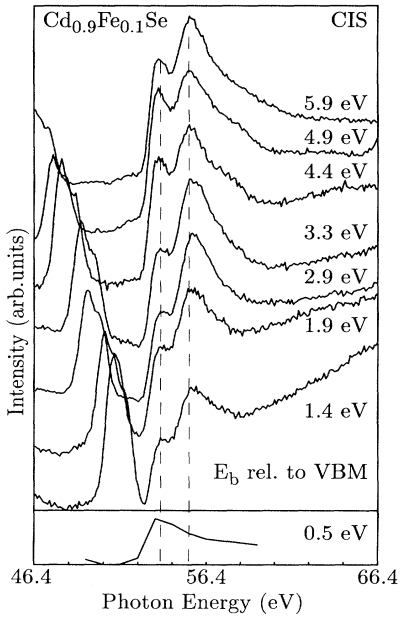


FIG. 2. Constant-initial-state (CIS) spectra of $Cd_{0.9}Fe_{0.1}Se$ for initial-state energies ($E_b$) in the valence-band region. The dashed lines denote the positions of the two resonance energies at 53.6- and 55.5-eV photon energy. The dispersive feature is a second-order Se 3*d* core emission. For the initial-state energy of 0.5 eV (bottom curve), we extracted the CIS spectrum from the EDC's of Fig. 1(a).

nances are observed here has to do with the nonvanishing orbital angular momentum of the $3d^6$ configuration of the $Fe^{2+}$ ion. The two resonances correspond to the following transitions:

$$3p^6 3d^6 4s^2\,{}^5D \rightarrow 3p^5 3d^7 4s^2\,{}^5P,{}^5F\ ,$$

$$3p^6 3d^6 4s^2\,{}^5D \rightarrow 3p^5 3d^7 4s^2\,{}^5D\ ,$$

which have been identified in atomic Fe at energies of 53.6 and 56.6 eV, respectively.[8] The multiplet splitting in our system is smaller because the Fe 3*d* electrons are delocalized through their hybridization with the Se 3*p* orbitals. For metallic Fe the splitting vanishes completely.[9]

It is evident from the relative intensities of the resonances in Fig. 2 that different parts of the valence-band spectrum couple differently to the two core excitations. This is particularly striking for the shoulder at the top of the valence bands (compare the spectrum for $E_b = 0.5$ eV in Fig. 2), which couples only to the ${}^5P,{}^5F$ states and not at all to the ${}^5D$ final state of the core excitation. These differences have to be taken into account when comparing the results of the CI calculation with the spectra. Without any further analysis, the CIS spectra of Fig. 2 illustrate that states with Fe 3*d* character are present throughout the valence-band spectra of $Cd_{1-x}Fe_xSe$ and not just in the most prominent structure at 3.8-eV binding energy, as might be inferred from Fig. 1.

One way to extract the contribution of Fe 3*d* states to the EDC's is to calculate difference spectra from EDC's taken on and off resonance. This is done for the $Cd_{0.9}Fe_{0.1}Se$ sample in Fig. 3, where we have chosen photon energies of 55.4 and 51.4 eV for the EDC's on and off resonance. The spectra are normalized to the photon flux, and the dashed line indicates the region where the subtraction of the very intense Cd 4*d* lines leads to some artificial features. Under the reasonable assumptions that the photoemission cross section of non-Fe 3*d* states does not vary appreciably over such a narrow energy range, the difference spectrum "56–52 eV" represents what we call the Fe 3*d*-derived partial valence-band spectrum of $Cd_{1-x}Fe_xSe$. A similar procedure using the $\hbar\omega = 53.6$-eV resonance leads to a partial valence-band spectrum "54–52 eV," in which different parts of the spectrum are weighted differently, as alluded to above. We shall return to this aspect in Sec. IV. Valence-band spectra similar to the ones presented here have been published by Taniguchi *et al.*[10] We find good agreement between the two sets of data, although there appear to be inconsistencies between the strength of the Fe-derived spectral features and the Fe content quoted in Ref. 10.

The correlation and hybridization of the Fe 3*d* states are also manifest in the satellite structures of the Fe core-level spectra. They shall therefore be discussed here as well. Figure 4 shows an x-ray photoemission spectroscopy (XPS) spectrum of the Fe 2*p* core-level region for a $Cd_{1-x}Fe_xSe$ sample with $x = 0.05$. The measurements were performed on an SSI ESCA spectrometer using monochromatized $Al K_\alpha$ photons with an energy of 1486.6 eV. Atomically clean sample surfaces have been prepared *in situ* by filing. The spectrum consists of the spin-orbit-split Fe $2p_{3/2}$ and $2p_{1/2}$ components, each accompanied by a satellite on the high-binding energy side. The overall shape of the two main components differs somewhat. For Ni compounds, it has been shown that, due to the Coster-Kronig decay of the $2p_{1/2}$ hole, the re-

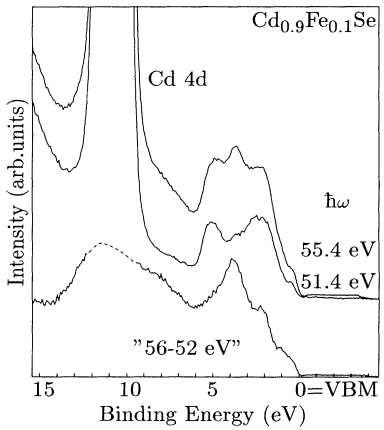


FIG. 3. The difference spectrum "56–52 eV" between the EDC's taken on ($\hbar\omega = 55.4$ eV) and off ($\hbar\omega = 51.4$ eV) resonance. The spectra are normalized to the photon flux. The dashed line indicates the region of the Cd 4*d* core line which causes artifacts in the subtraction procedure. The difference spectrum represents the Fe 3*d*-derived partial valence-band spectrum of $Cd_{0.9}Fe_{0.1}Se$.

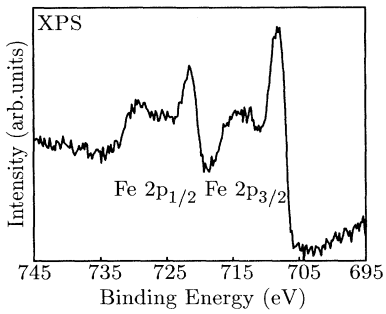


FIG. 4. The XPS spectrum of the Fe $2p$ core-level region of $Cd_{0.95}Fe_{0.05}Se$ taken with Al $K\alpha$ photons ($\hbar\omega = 1486.6$ eV). The spin-orbit splitting into $2p_{3/2}$ and $2p_{1/2}$ components and additional satellites is clearly seen. A linear background has been subtracted from the spectrum.

laxation of the valence electrons and the decay of the core hole cannot be treated independently. This leads to strong distortions of the $2p_{1/2}$ spectrum.[11] In our analysis, we will therefore concentrate on the undisturbed $2p_{3/2}$ line.

## III. CI CALCULATIONS

Because of the highly correlated nature of the Fe $3d$ states, a direct interpretation of the partial valence-band spectra in terms of a ground-state partial density of states is not possible. In a first approximation it suffices to consider the energetic distribution of the $3d^5$ final-state multiplets that can be reached via photoemission from the Fe $3d^6$ ground state. This approach has been shown to work reasonably well in ionic compounds of transition or $4f$ metals.[12] However, in $Cd_{1-x}Fe_xSe$ with its considerable covalency, one has to consider the possibility of a charge transfer between the Fe $3d$ and the band states as well. The most important of these hopping matrix elements, namely the ones between Fe $3d$ and Se $3p$ states of the immediate neighbors, are included in the present configuration-interaction scheme which considers an isolated $[Fe^{2+}Se_4^{2-}]^{6-}$ cluster. This type of CI scheme was first introduced by Fujimori and Minami.[3] The success of this approach in interpreting the valence-band spectra of NiO (Ref. 13) and $Cd_{1-x}Mn_xTe$,[4] for example, encourages us to use the same scheme for the interpretation of our data. Its main drawback, the neglect of band dispersion in the anion states, is apparently of secondary importance compared to the intra-atomic Coulomb energy and the Fe $3d \rightarrow$ Se $3p$ hybridization.

In $Cd_{1-x}Fe_xSe$, the Fe ion is tetrahedrally surrounded by four Se ions in the wurtzite structure, and we therefore start with a $[FeSe_4]^{6-}$ cluster in which the Fe is tetrahedrally surrounded by four Se atoms. The ground state of the $Fe^{2+}$ ion has $^5E$ symmetry: Fe $3d^6{:}e^3(^2E)t_2^3(^4A_2)^5E$. Capital letters refer to the irreducible representations of the tetrahedral point group $T_d$, and the superscripts denote the spin multiplicity $(2S+1)$.

In addition to this "normal" ground state, the CI theory considers hybridized states in which an electron is transferred from a ligand to a Fe $3d$ orbital. Only those states will, of course, contribute to the ground states that have the same symmetry as the "normal" ground state, in this case $^5E$. The CI ground state may thus be written as follows:

$$\psi_g(^5E) = a_0|e^3t_2^3\,^5E\rangle + a_{11}|e^4t_2^3(^4A_2)\underline{L}_\sigma\,^5E\rangle + a_{21}|e^3t_2^4(^4T_1)\underline{L}_\pi\,^5E\rangle + a_{22}|e^3t_2^4(^4T_2)\underline{L}_\pi\,^5E\rangle\ , \tag{1}$$

where $\underline{L}_{\pi,\sigma}$ denotes a hole state on the ligand, depending on whether the electron is being transferred to the Fe via a $\sigma$ or a $\pi$ bond.

To calculate the energy of the ground state and the amplitudes $a_{ij}$, one has to diagonalize the following Hamiltonian:

$$H = \begin{pmatrix} E_6 & v_\sigma & \sqrt{3}v_\pi & \sqrt{3}v_\pi \\ v_\sigma & E_6+\delta E_A+\Delta(^4A_2) & 0 & 0 \\ \sqrt{3}v_\pi & 0 & E_6+\delta E_A+\Delta(^4T_1) & 0 \\ \sqrt{3}v_\pi & 0 & 0 & E_6+\delta E_A+\Delta(^4T_2) \end{pmatrix} . \tag{2}$$

Here $E_6$ is the energy of the "normal" $|d^6\rangle$ ground-state configuration, $\delta E_A$ is the charge-transfer energy between the ligand orbital and the $3d$ orbital which can be written as $\delta E_A = \epsilon_d - \epsilon_L + U$, where $\epsilon_d$ and $\epsilon_L$ are the ionization energies of $d$ and the ligand electrons, respectively, and $U$ denotes the correlation energy of the $3d$ shell. $v_\sigma$ and $v_\pi$ are the effective transfer integrals, e.g., $v_\sigma = \langle d^6|H|d^7\underline{L}_\sigma\rangle$, and $\Delta(^{2s+1}\Gamma)$ is the energy of the configuration with symmetry $^{2s+1}\Gamma$ relative to the corresponding "normal" configuration. The values for $\Delta(^{2s+1}\Gamma)$ have been taken from Ref. 14 using the Racah parameters and the electrostatic part of the crystal-field splitting, $\Delta_{CF}$, from Table I. Parameters such as the "normal" ground-state energy $E_6$ which appear in all diagonal matrix elements lead only to an offset of the energy scale and are without consequences for our considerations.

Dipole-allowed final states may have symmetries $^6A_1$, $^4A_1$, $^4A_2$, $^4E$, $^4T_1$, and $^4T_2$.[16] Here we again consider three configurations which correspond to the removal of one $d$ electron from the ground state:

$$\psi_f(^{2S+1}\Gamma) = b_0|d^5\,^{2S+1}\Gamma\rangle + \sum_i b_{1i}|d^6\underline{L}_\sigma\,^{2S+1}\Gamma\rangle + \sum_j b_{2j}|d^6\underline{L}_\pi\,^{2S+1}\Gamma\rangle\ . \tag{3}$$

TABLE I. Parameters used for the CI calculation of the partial valence-band spectra and the XPS core-level spectrum. G.S. and F.S. refer to the ground and final states of the Fe ion, respectively.

| | VB spectra | |
|---|---|---|
| $\delta E_A$ | 4 eV | |
| $\delta E_B$ | −3 eV | |
| $U$ | 7 eV | |
| $v_\sigma = -\sqrt{3}(pd\sigma)$ | 1.82 eV | Ref. 15 |
| $v_\pi = -2(pd\pi)$ | −0.95 eV | Ref. 15 |
| **Racah parameter** | **G.S. $Fe^{2+}$** | **F.S. $Fe^{3+}$** |
| $A$ | −0.213 eV | −0.267 eV |
| $B$ | 0.114 eV | 0.126 eV |
| $C$ | 0.501 eV | 0.595 eV |
| $\Delta_{CF}$ | 0.4 eV | |
| | **XPS spectrum** | |
| $T$ | 1.6 eV | |
| $U$ | 5.5 eV | $U/Q = 0.7$ (Ref. 19) |
| $Q$ | 7.8 eV | |
| $\Delta$ | 4 eV | |

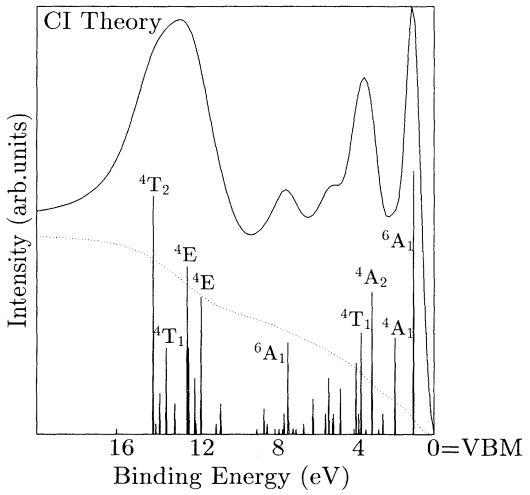


FIG. 5. The partial valence-band spectrum of Fe in a $[FeSe_4]^{6-}$ cluster calculated with CI theory. The line spectrum in which the main lines are labeled with their irreducible representations has been convoluted with Lorentzian and Gaussian functions to simulate the lifetime broadening and the resolution of the experiment, respectively. Also, a background according to the recipe given by Shirley (Ref. 18) has been added (dotted line) to facilitate comparison with experiment.

The Hamiltonians which have to be diagonalized separately for each symmetry $\Gamma$ are similar to the one shown above for the ground state. For the charge-transfer energy, we now have $\delta E_B = \epsilon_d - \epsilon_L$ without the correlation energy $U$. The reason is that we consider only transitions $|d^6\rangle \rightarrow |d^5\rangle$, $|d^7\underline{L}_{\sigma,\pi}\rangle \rightarrow |d^6\underline{L}_{\sigma,\pi}\rangle$, in which one $d$ electron has been removed.

In order to calculate the partial valence-band spectra, we have to calculate relative intensities as well as the appropriate final-state energies. This requires us to calculate transition matrix elements such as

$$I = \left| a_0 b_0 \langle d^6 | \mathbf{A}\cdot\mathbf{p} | d^5 \rangle + \sum_i a_{1i} b_{1i} \langle d^7\underline{L}_\sigma | \mathbf{A}\cdot\mathbf{p} | d^6\underline{L}_\sigma \rangle + \sum_j a_{2j} b_{2j} \langle d^7\underline{L}_\pi | \mathbf{A}\cdot\mathbf{p} | d^6\underline{L}_\pi \rangle \right|^2 , \quad (4)$$

where $\mathbf{A}$ refers to the vector potential of the photon field and $\mathbf{p}$ to the momentum operator, respectively. The coefficients $a_{nk}, b_{nk}$ are the components of the initial- and final-state eigenvectors, respectively. The transition matrix elements are taken from Ref. 16 or have been calculated using fractional parentage coefficients.[14] Details concerning the matrix elements can be found elsewhere.[17]

In order to compare the theoretical spectra with the measurements, we convolute the line spectra obtained in the CI calculation with a Gaussian of 0.8-eV full width at half maximum (FWHM) and a Lorentzian function to account for the finite experimental resolution and the lifetime of the final states, respectively. The width of the Lorentzian scales with the binding energy $E_b$ according to $0.1E_b$, to account for the increasing imaginary part of the hole self energy. Figure 5 shows a partial valence-band spectrum calculated in this way with the parameters of Table I, after a background following Shirley[18] has been added.

In order to evaluate the XPS spectrum of Fig. 4, we use an approach similar to that for the valence-band spectra.[19] The ground state is assumed to be a mixture of the five configurations $|d^6\rangle$, $|d^7\underline{L}\rangle$, $|d^8\underline{L}^2\rangle$, $|d^9\underline{L}^3\rangle$, and $|d^{10}\underline{L}^4\rangle$. The former distinction between $\underline{L}_\sigma$ and $\underline{L}_\pi$ states has been neglected here. The final states consist of the configurations $|cd^6\rangle$, $|cd^7\underline{L}\rangle$, $|cd^8\underline{L}^2\rangle$, $|cd^9\underline{L}^3\rangle$, and $|cd^{10}\underline{L}^4\rangle$, where $c$ denotes a core hole. In order to obtain the eigenvalues and eigenvectors belonging to the hybridized states, we have to diagonalize the following Hamiltonians for the ground and the final states, respectively:

$$H_g = \begin{pmatrix} 0 & \sqrt{2}T & 0 & 0 & 0 \\ \sqrt{2}T & \Delta & \sqrt{2}T & 0 & 0 \\ 0 & \sqrt{2}T & 2\Delta+U & \sqrt{2}T & 0 \\ 0 & 0 & \sqrt{2}T & 3\Delta+3U & \sqrt{2}T \\ 0 & 0 & 0 & \sqrt{2}T & 4\Delta+6U \end{pmatrix} , \quad (5)$$

$$H_f = \begin{bmatrix} 0 & \sqrt{2}T & 0 & 0 & 0 \\ \sqrt{2}T & \Delta-Q & \sqrt{2}T & 0 & 0 \\ 0 & \sqrt{2}T & 2(\Delta-Q)+U & \sqrt{2}T & 0 \\ 0 & 0 & \sqrt{2}T & 3(\Delta-Q)+3U & \sqrt{2}T \\ 0 & 0 & 0 & \sqrt{2}T & 4(\Delta-Q)+6U \end{bmatrix} , \quad (6)$$

where $Q$ is the core-hole $d$-electron Coulomb attraction and $\Delta$ the charge-transfer energy which corresponds to $\delta E_A$ of the valence-band calculation. $T$ is the effective transfer integral without distinction between the different methods of transfer.

With the ground and final states so obtained, we again calculate theoretical core-level spectra using the dipole matrix elements. In Fig. 6, we compare the measured (dotted line) and the calculated Fe $2p_{3/2}$ spectra using the parameters listed in Table I. The theoretical line spectrum which is also shown in Fig. 6 has again been convoluted with Lorentzian and Gaussian functions. For the lifetime broadening, we used a Lorentzian with FWHM depending on the energy separation $\Delta E$ between the satellites and the main peak. The FWHM thus has the form

$$\Gamma_n = \Gamma_0(1+\alpha\Delta E) ,$$

where $\Gamma_0$ reflects the broadening of the main peak and $\alpha$ is a constant.[20] For our calculation, we used $\Gamma_0 = 1.2$ eV and $\alpha = 0.2$. The Gaussian function represents the experimental broadening and the FWHM was assumed to be 1 eV. Figure 6 also shows the background which has been added to the theoretical spectrum using the same procedure as for the valence-band calculations.

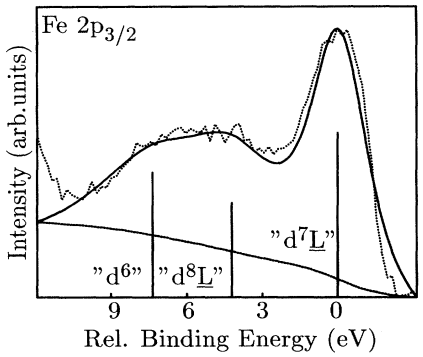


FIG. 6. A comparison between the experimental XPS spectrum of the Fe $2p_{3/2}$ core line (dotted line) and the CI calculation. Also shown is the underlying line spectrum which has been convoluted with a Lorentzian function with a FWHM of $\Gamma_n = \Gamma_0(1+\alpha\Delta E)$, with $\Gamma_0 = 1.2$ eV and $\alpha = 0.2$, respectively, representing the lifetime broadening, and a Gaussian function with a FWHM of 1 eV representing the finite resolution. The three lines are labeled with their major configuration. The background which has been added to the theoretical spectrum is shown as the dashed line.

## IV. DISCUSSION

The difference spectra of Fig. 7 exhibit remarkable differences for the two resonance energies. This effect is due to the different coupling strengths of the core excitation to the valence $d$ states. The calculation discussed in Sec. III yields only the spectrum of the direct photoemission process. For a realistic comparison we have to take the coupling strengths of individual final states to the core absorption into account as well. These coupling strengths have been extracted from photoemission measurements on atomic Fe,[8] and they are listed in Table II for all relevant final states. When applied to our theoretical spectrum of Fig. 5, these weighting factors yield two different partial valence-band spectra for Fe in $Cd_{1-x}Fe_xSe$, one for each resonance energy. They are shown in Fig. 7 together with the corresponding experimental results. Whereas without these coupling factors no resemblance between the experimental and the calcu-

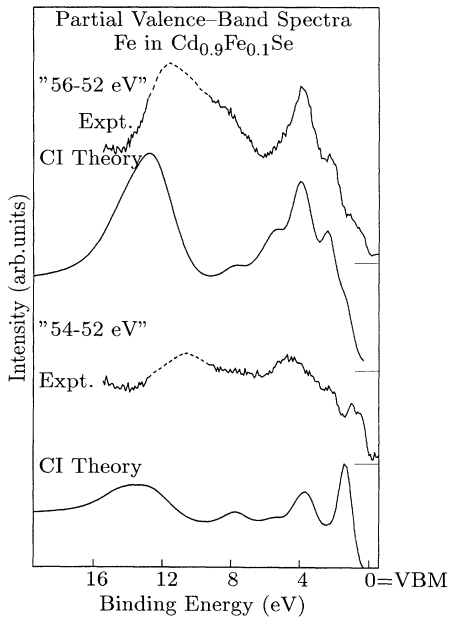


FIG. 7. A comparison between the measured partial valence-band spectra and the results of the CI calculation for the two resonances. Different coupling strengths of the final states of the CI calculation to the two Fe $3p$-$3d$ resonances ($3p^63d^6\,{}^5D \rightarrow 3p^53d^7\,{}^5P, {}^5F$ at about 53.6 eV and $3p^63d^6\,{}^5D \rightarrow 3p^53d^7\,{}^5D$ at about 55.5 eV) have been taken into account using weighting factors obtained from free atom data (Ref. 8). Again, the model spectra have been broadened with Lorentzian and Gaussian functions as explained in the text.

TABLE II. Weighting factors for the final states labeled with their irreducible representation (irr. rep.) for the two resonance energies as extracted from Ref. 8.

| irr. rep. | Resonance at 53.6 eV | Resonance at 55.5 eV |
|---|---|---|
| $^6A_1$ | 1 | 0.15 |
| $^4A_1$ | 0.63 | 1 |
| $^4A_2$ | 1 | 0.46 |
| $^4E$ | 0.63 | 1 |
| $^4T_1$ | 0.63 | 1 |
| $^4T_2$ | 0.65 | 0.3 |

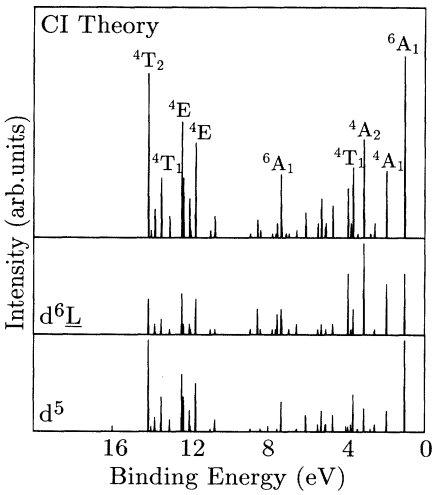


FIG. 8. The decomposition of the Fe CI final-state spectrum into contributions with different $3d$ electron counts. Only the main peaks are labeled according to their irreducible representation of the point group $T_d$.

lated partial valence-band spectra could be obtained, there is now reasonable agreement between the two. This is particularly so for the $^6A_1$ state, that is, according to our calculation, responsible for the abrupt change in the VBM with the introduction of Fe. It shows up strongly in the 53.6-eV resonance and as a mere shoulder in the 55.5-eV resonance, as observed experimentally, thus lending support to the ordering of final states as calculated. It is only on the basis of this comparison that we were able to obtain the parameters of our CI calculation as they are listed in Table I. Comparing our parameters with those published for similar systems, we find that our correlation energy of $U=7$ eV compares favorably with $U=8$ eV for Fe in $Fe_2O_3$,[13] $U=7$ eV for Ni in NiO,[3] and with $U=8$ eV for Mn in $Cd_{1-x}Mn_xTe$.[4]

Aside from the correlation energy, our calculation also yields information about the covalency of the Fe-Se bond. The ground state turns out to be a mixture of 83% $|d^6\rangle$ and 17% $|d^7\underline{L}\rangle$ configuration, which corresponds to an effective number of electrons on the Fe ions of 6.16. The ground state is thus correctly described as a $Fe^{1.8+}$ ion.

Just looking at the partial valence-band spectra, one would classify spectral features as is usually done for $3d$ transition metals, into the "main," i.e., fully screened $|d^6\underline{L}\rangle$ contribution at the top 5 eV, and into the "satellite," the broad structure centered around 10-eV binding energy which would correspond to the unscreened $|d^5\rangle$ configurations. This state of affairs seems also to hold for the CI calculations when we identify the group of final states centered around 13 eV with the "satellite."

However, the nature of final states in terms of their character as screened ($|d^6\underline{L}\rangle$) and unscreened ($|d^5\rangle$) may be discussed more rigorously with reference to Fig. 8. Here the final-state spectrum of Fig. 5 is decomposed into contributions from $|d^5\rangle$ and $|d^6\underline{L}\rangle$ configurations, respectively. The weight of the two contributions is indeed distributed as expected: $|d^5\rangle$ configurations tend to be more concentrated around 13 eV, whereas the $|d^6\underline{L}\rangle$ configurations dominate in the top 5 eV. The separation is, however, far from being as clearcut as, for example, in systems containing Mn.[4] Both configurations contribute significantly over the whole spectral region. A particularly conspicuous case is again the $^6A_1$ at the VBM, which actually has more $|d^5\rangle$ contributions than $|d^6\underline{L}\rangle$. The reason for this can be found in the extremely stable configuration formed by the half-filled shell, as can be deduced from Hund's rule.

The evaluation of the XPS spectrum also yields information about the correlation energy $U$ and the ground-state properties. With our choice of parameters used to calculate the spectrum of Fig. 6, we obtain a correlation energy $U=5.5$ eV. This is smaller than the one derived from the valence-band calculations, but it is again comparable to results for other transition-metal oxides.[21] According to Zaanen, Westra, and Sawatzky,[19] the calculated values of $U$ depend on the special choice of the Hamiltonian which is by necessity made to treat the particular problem most "effectively"; therefore the values derived from different experiments are not necessarily comparable.

For the ground-state configuration of the Fe ions, we obtain from the XPS calculations a mixture of 81% $|d^6\rangle$, 18% $|d^7\underline{L}\rangle$, and 1% $|d^8\underline{L}^2\rangle$, leading again to a number of 6.2 $d$ electrons on the Fe ion. The three main final states are made up in different proportion from the five final-state configurations considered. In Fig. 6, we have labeled the final states according to their main configuration. We find that the state wherein one electron is transferred to screen the core hole is the stablest state. It is interesting to note that the state predominantly made up of configurations containing two screening electrons is less tightly bound than the "$d^6$" state.

## V. CONCLUSION

By means of resonant photoemission and the calculation of difference spectra, we obtained partial Fe $3d$-derived valence-band spectra for $Cd_{1-x}Fe_xSe$. These spectra reveal Fe contributions over the whole valence band. In particular, the top of the valence bands changes its character with the introduction of Fe from Cd and Se $sp$-like to Fe $3d$-like.

On the basis of configuration interaction (CI) calculations for a $[FeSe_4]^{6-}$ cluster, we identified the Fe-derived

valence-band states and obtained additional information about the ground and the final states, such as the correlation energy in the $3d$ shell and the effective charge state of Fe, which turned out to be $+1.8$.

An analysis of the Fe $2p$ core-level spectrum again using a CI calculation scheme corroborates the UPS-derived values for the ground-state configuration of Fe, but yields a smaller value for the $d$-shell correlation energy.

Our results, finally, bear also on the optical data of $Cd_{1-x}Fe_xSe$. The addition of Fe to CdSe leads to a shoulder in the absorption spectrum which moves the onset of absorption to lower energy by about 0.5 eV.[22] The corresponding transition was identified with a charge-transfer transition from Fe $3d$ states to the conduction band. On the basis of our measurements, we assign the final state in this transition to the $Fe^{3+}$ configuration with ${}^6A_1$ symmetry. This is, according to our measurements and the CI calculation, the $Fe^{3+}$ configuration with the lowest excitation energy. It is lower by about 0.5 eV than the threshold for CdSe band states. In this respect $Cd_{1-x}Fe_xSe$ differs qualitatively from $Cd_{1-x}Mn_xTe$, where the Mn excitations required energies larger than those of the top valence states of the host compound.[23]

## ACKNOWLEDGMENTS

This work has been supported by the Bundesministerium für Forschung und Technologie under Contract No. 2.3-D19. Thanks are due to B. A. Orlowski from the Polish Academy of Sciences, for providing the samples and helping us with the experiments, to the staff of BESSY synchrotron, especially W. Braun, to J. Faul for assistance with the measurements and for fruitful discussions, and to R. Graupner for performing the XPS measurements.

[1]N. Samarth and J. K. Furdyna, Proc. IEEE **78**, 990 (1990); J. K. Furdyna, J. Appl. Phys. **53**, 7637 (1982).

[2]R. R. Galazka, in *Physics of Semiconductors 1978,* edited by B. L. H. Wilson, IOP Conf. Proc. No. 43 (Institute of Physics and Physical Society, Bristol, 1979); N. B. Brandt and V. V. Moshchalkov, Adv. Phys. **33**, 193 (1984).

[3]A. Fujimori and F. Minami, Phys. Rev. B **30**, 957 (1984).

[4]L. Ley, M. Taniguchi, J. Ghijsen, and R. L. Johnson, Phys. Rev. B **35**, 2839 (1987).

[5]R. C. G. Leckey and J. D. Riley, Appl. Surf. Sci. **22/23**, 196 (1985).

[6]E. Dynowska, A. Sarem, B. Orlowski, and A. Mycielski, Mater. Res. Bull. **25**, 1109 (1990).

[7]U. Fano, Phys. Rev. **124**, 1866 (1961).

[8]E. Schmidt, H. Schröder, B. Sonntag, H. Voss, and H. E. Wetzel, J. Phys. B **16**, 2961 (1983).

[9]R. J. Lad and V. E. Henrich, Phys. Rev. B **39**, 13 478 (1989).

[10]M. Taniguchi, Y. Ueda, I. Morisada, Y. Murashita, T. Ohta, I. Souma, and Y. Oka, Phys. Rev. B **41**, 3069 (1990).

[11]J. Zaanen and G. A. Sawatzky, Phys. Rev. B **33**, 8074 (1986).

[12]A. Fujimori, Phys. Rev. B **27**, 3992 (1983); **28**, 4489 (1983).

[13]A. Fujimori, M. Saeki, N. Kimizuka, M. Taniguchi, and S. Suga, Phys. Rev. B **34**, 7318 (1986).

[14]J. S. Griffith, *The Theory of Transition-Metal Ions* (Cambridge University Press, Cambridge, 1971).

[15]L. F. Mattheiss, Phys. Rev. B **5**, 290 (1972).

[16]P. S. Bagus, J. L. Freeouf, and D. E. Eastman, Phys. Rev. B **15**, 3661 (1977).

[17]R. Denecke, Diplomarbeit, Universität Erlangen-Nürnberg, 1991 (unpublished).

[18]D. A. Shirley, Phys. Rev. B **5**, 4709 (1972).

[19]J. Zaanen, C. Westra, and G. A. Sawatzky, Phys. Rev. B **33**, 8060 (1986).

[20]A. E. Bocquet, T. Mizokawa, T. Saitoh, H. Namatame, and A. Fujimori, Phys. Rev. B **46**, 3771 (1992).

[21]J. Park, S. Ryu, M. Han, and S. J. Oh, Phys. Rev. B **37**, 10 867 (1988).

[22]A. Mycielski, P. Dzwonkowski, B. Kowalski, B. A. Orlowski, M. Dobrowolski, M. Arciszewska, W. Dobrowolski, and J. M. Baranowski, J. Phys. C **19**, 3605 (1986).

[23]M. Taniguchi, L. Ley, R. L. Johnson, J. Ghijsen, and M. Cardona, Phys. Rev. B **33**, 1206 (1986).